


Versatility of the green microalga cell vacuole function as revealed by analytical transmission electron microscopy

Anastasia Shebanova¹ · Tatiana Ismagulova¹ · Alexei Solovchenko^{1,2,3}  · Olga Baulina¹ · Elena Lobakova¹ · Alexandra Ivanova^{4,5} · Andrey Moiseenko¹ · Konstantin Shaitan¹ · Vladimir Polshakov⁶ · Ladislav Nedbal⁷ · Olga Gorelova¹

Received: 15 June 2016 / Accepted: 8 September 2016 / Published online: 27 September 2016
© Springer-Verlag Wien 2016

Abstract Vacuole is a multifunctional compartment central to a large number of functions (storage, catabolism, maintenance of the cell homeostasis) in oxygenic phototrophs including microalgae. Still, microalgal cell vacuole is much less studied than that of higher plants although knowledge of the vacuolar structure and function is essential for understanding physiology of nutrition and stress tolerance of microalgae. Here, we combined the advanced analytical and conventional transmission electron microscopy methods to obtain semi-quantitative, spatially resolved at the subcellular level information on elemental composition of the cell vacuoles in several free-living and symbiotic chlorophytes. We obtained a detailed record of the changes in cell and vacuolar ultrastructure in response to

environmental stimuli under diverse conditions. We suggested that the vacuolar inclusions could be divided into responsible for storage of phosphorus (mainly in form of polyphosphate) and those accommodating non-protein nitrogen (presumably polyamine) reserves, respectively.

The ultrastructural findings, together with the data on elemental composition of different cell compartments, allowed us to speculate on the role of the vacuolar membrane in the biosynthesis and sequestration of polyphosphate. We also describe the ultrastructural evidence of possible involvement of the tonoplast in the membrane lipid turnover and exchange of energy and metabolites between chloroplasts and mitochondria. These processes might play a significant role in acclimation in different stresses including nitrogen starvation and extremely high level of CO₂ and might also be of importance for microalgal biotechnology. Advantages and limitations of application of analytical electron microscopy to biosamples such as microalgal cells are discussed.

Handling Editor: Tsuneyoshi Kuroiwa

Electronic supplementary material The online version of this article (doi:10.1007/s00709-016-1024-5) contains supplementary material, which is available to authorized users.

✉ Alexei Solovchenko
solovchenko@mail.bio.msu.ru

- ¹ Lomonosov Moscow State University, Moscow, Russia
- ² Timiryazev Institute of Plant Physiology, Russian Academy of Sciences, Moscow, Russia
- ³ Faculty of Biology, Moscow State University, Leninskie Gori 1/12, 119234 GSP-1 Moscow, Russia
- ⁴ Komarov Botanical Institute, Russian Academy of Sciences, St. Petersburg, Russia
- ⁵ St. Petersburg State University, St. Petersburg, Russia
- ⁶ Faculty of fundamental medicine, Lomonosov Moscow State University, Moscow, Russia
- ⁷ Institute of Bio- and Geosciences / Plant Sciences (IBG-2), Forschungszentrum Jülich, Jülich, Germany

Keywords Analytical electron microscopy · Microalgae · Nitrogen · Phosphorus · Polyphosphate · Stress responses · Vacuole

Abbreviations

| | |
|------------|---|
| DAPI | 4',6-diamidino-2-phenylindole |
| EDX | Energy-dispersive X-ray spectroscopy |
| EELS | Electron energy loss spectroscopy |
| EFTEM | Energy-filtered transmission electron microscopy |
| EMS | Epichloroplast membrane structure |
| HAADF-STEM | High angle annular dark-field scanning transmission electron microscopy |
| NMR | Nuclear magnetic resonance |

| | |
|-------|---|
| PolyP | Polyphosphate(s) |
| STEM | Scanning transmission electron microscopy |
| TEM | transmission electron microscopy |

Introduction

Vacuole is a multifunctional cell compartment central to the functions of catabolism, storage, the cell homeostasis maintenance, as well as to development and detoxication in green plants including microalgae (Marty 1999). Study of the structure and function of the vacuole provides essential insights into the mechanisms of physiological plasticity of cells under environmental and biotic stresses. However, the microalgal cell vacuoles are much less studied in comparison with those of higher plant cells. Compared to higher plants, this opportunity has so far not been adequately addressed in microalgae where more studies of cellular vacuoles are needed.

The membrane (tonoplast) of large vacuoles of green algae (Bethmann et al. 1995) hosts transport mechanisms resembling those of terrestrial plants. Thus, the tonoplast of a chlorophyte *Chlorococcum littorale* (Sasaki et al. 1999) as well as the membrane of lytic vacuoles of *Chlamydomonas reinhardtii* (Robinson et al. 1998), including the electron-dense vacuoles (Ruiz et al. 2001), harbors pyrophosphatase (H^+ -PPase), vacuolar ATPase (V-ATPase) (Maeshima 2000), and acid phosphatase (Matagne et al. 1976). The vacuoles filled with electron-dense matter are actually typical of many microalgae. These organelles are believed to function as a depot of polyphosphates (PolyP) and divalent cations in the cell (Docampo et al. 2005; Docampo and Huang 2016). Becker (2007) considered the presence of the enzymatic machinery for P_i transport/energy transformation in the vacuolar membranes of *Ch. reinhardtii* to indicate involvement in the catabolism of polyphosphates, similar to function of lysosomes in animal and higher plant cells (Hedrich et al. 1989). These organelles are believed to function as depots of polyphosphates.

Interest in vacuolar functions in the microalgal cell has been further stimulated by the recent progress in microalgal biotechnology (Gong et al. 2011; Lam and Lee 2012; Ray et al. 2013). Biosynthesis of diverse high-value compounds by microalgal cells is stimulated by stress, particularly by nutrient limitation, in which vacuoles play an essential role. Also, potentially involving vacuoles is biocapture of nutrients from waste streams (Pittman et al. 2011). Nutrient uptake depends on the cell quota of nitrogen and/or phosphorus storage, part of which involves vacuoles (Lourenço et al. 1998; Powell et al. 2009; Solovchenko et al. 2016b).

Functionalities of microalgal vacuoles have so far been only rarely approached on a subcellular level (Sviben et al. 2016; Ota et al. 2016). A unique opportunity for new insights on this level is offered by analytical transmission electron microscopy (TEM) that is well established in material science

but much less exploited in biology. At the origins of this new method, conventional TEM has been first established as powerful tool in life science for investigation of morphology and ultrastructure of various objects including cell vacuoles. Later, it was extended with analytical capabilities of energy-dispersive X-ray spectroscopy (EDX) or electron energy loss spectroscopy (EELS) that complement TEM images of the specimen with its elemental content and composition with a nanoscale resolution (Egerton 2009; Brydson et al. 2014). In the past two decades, new highly sensitive detectors and advanced data analysis algorithms further advanced capacity of analytical TEM to perform spatially resolved elemental analysis of biological objects (Aronova and Leapman 2012; Warley 2016). Analytical TEM became a very potent tool for detecting metals such as Ca (Nishikawa et al. 2003), Cr (Millach et al. 2015), Cu, and Pb (Burgos et al. 2013) in green microalgae at a subcellular level. This approach is significantly more difficult when “light” elements such as N or P in microalgal cells have to be detected. Further complicating factor may be the focus on vacuole where the target elements may be sometimes present at low concentrations and samples can be unstable or hard to prepare without altering the vacuolar composition. Hence, the reports on the distribution and elemental composition of native microalgal cell structures under physiological conditions are scarce. Only recently, EDX was successfully applied by Ota et al. (2016) to study the relationship between PolyP accumulation and occurrence of the electron-dense bodies in the sulfur-deprived chlorophyte *Parachlorella kessleri* NIES-2152. Successful application of TEM coupled with EELS is exemplified by the analysis of Fe, Al, and Si in the cell wall and vacuolar inclusions of snow algae (Lütz-Meindl and Lütz 2006), study of Ca binding by pectin-like carbohydrates in chlorophytes (Eder and Lütz-Meindl 2008; 2010), study of coccolith-producing compartment inside the cells of unicellular marine algae *Emiliania huxleyi* (Sviben et al. 2016), and finding the sites of H_2O_2 generation via peroxidase reaction with $CeCl_3$ in osmotically stressed *Micrasterias* cells (Darehshouri and Lütz-Meindl 2010).

In the present work, we focus on the vacuoles of model free-living and symbiotic chlorophytes grown under various conditions (Table 1). These organisms contain ample vacuoles with inhomogeneous electron density filling (Gorelova et al. 2015a) that may represent polyphosphate reserves (Becker 2007). One of these microalgae, *Desmodesmus* sp. IPPAS S-2014, was characterized in our laboratory previously under different growth conditions (irradiance, nutrient availability, elevated CO_2 stress; see Solovchenko et al. 2014; 2015; 2016b; Gorelova et al. 2015b; Baulina et al. 2016) and represents an adequate model for study of the changes in the ultrastructure and elemental composition of the cell vacuoles in responses to these factors. However, the data on elemental composition resolved at the subcellular level, in particular for the vacuoles and

Table 1 Microalgal strains and cultivation conditions

| Microalgal strain | Origin | Cultivation conditions ^a | Designation |
|--|---|---|------------------------|
| <i>Chlorella vulgaris</i> CCALA 256 | The Culture Collection of Autotrophic Organisms, Institute of Botany Czech Acad. Sci., Třeboň, Czech Republic (CCALA) | “2.5%CO ₂ , -P” “2.5%CO ₂ , +P” | <i>C. vulgaris</i> 256 |
| <i>Parachlorella kessleri</i> CCALA 251 | CCALA | “2.5%CO ₂ , -P” “2.5%CO ₂ , +P” | <i>P. kessleri</i> 251 |
| <i>C. vulgaris</i> IPPAS C-1 | K.A. Timiryazev Institute of Plant Physiology—IPPAS, Russian Acad. Sci | “2.5%CO ₂ , -P” “2.5%CO ₂ , +P” | <i>C. vulgaris</i> C-1 |
| <i>Desmodesmus</i> sp. IPPAS S-2014 ^b | IPPAS | +N” “Air, +N” “Air, -N” “20%CO ₂ , +N” “20%CO ₂ , -N” “100%CO ₂ , +N” “100%CO ₂ , -N” | <i>Desmodesmus</i> sp. |
| <i>Acutodesmus obliquus</i> 46 | Algal collection of Bioengineering Department, Biological Faculty, Lomonosov MSU | +N” “Air, +N” “Air, -N” “20%CO ₂ , +N” “20%CO ₂ , -N” “100%CO ₂ , +N” “100%CO ₂ , -N” | <i>A. obliquus</i> 46 |

^a No bubbling or bubbling with air (Air) (0.04 % CO₂); +N or +P, complete medium; -P, P-free medium; -N, N-free medium. For the CO₂-enriched cultures, CO₂ volume (STP) percentages in the air-gas mixture passed through a 0.22- μ m bacterial filter (Merck-Millipore, Billerica, MA, USA) are specified. Pure (99.999 %) CO₂ from cylinders was used. For more detail, see text

^b A symbiotic strain *Desmodesmus* sp. IPPAS S-2014 (referred earlier as *Desmodesmus* sp. 3Dp86E-1) from a hydroid *Dynamena pumila* (Gorelova et al. 2015a)

inclusions harbored by these structures, are missing so far. In the present work, we complemented the TEM images with two analytical TEM techniques, EDX and EELS. The data on the observed ultrastructural and physiological responses linked with the dynamics of the elemental content allowed us to formulate hypothesis on the roles of vacuolar compartments in microalgae under stress. Further, we also demonstrate that the modern analytical TEM-based approaches reveal a plethora of valuable information at subcellular level making it possible to gain a deep insight into the roles of vacuolar compartment in the P and N metabolism and in homeostasis of microalgal cells. In conclusion, we summarize essentials for a successful application of the analytical TEM methods to microalgal cells.

Material and methods

Algal strains and cultivation conditions

The following algae were used in the investigation: *Chlorella vulgaris* CCALA 256, *Chlorella vulgaris* IPPAS C-1, *Parachlorella kessleri* CCALA 251, *Desmodesmus* sp. IPPAS S-2014, *Acutodesmus obliquus* 46. The key information about the studied algal strains, their designations, and cultivation conditions is summarized in Table 1. The cultures of *C. vulgaris* 256, *P. kessleri* 251, and *C. vulgaris* C-1 were subjected to P

starvation; the cultures of *Desmodesmus* sp. and *A. obliquus* 46 were grown at different N availability. The cultivation in P- and/or N-free was carried out as follows. The cells of the corresponding pre-culture (see below) were harvested by centrifugation (1200 \times g for 5 min), twice washed in fresh P- or N-free or N-containing medium, respectively, and resuspended in the corresponding (-P or -N or +N) medium to the initial chlorophyll (Chl) concentration content of 25 mg/L Chl.

The pre-cultures of *C. vulgaris* 256, *P. kessleri* 251, and *C. vulgaris* C-1 were transferred to 5 L of phosphorus-free Tamiya medium (Tamiya 1957) in a V-bag bioreactor (NOVAgreen®) inside a greenhouse. The cultures were grown under natural solar illumination (March in Jülich, Germany) combined with a supplemental continuous illumination by fluorescent tubes (Sylvania T8 GroLux F18W/GRO, Belgium) that added 250 μ mol PAR photons $m^{-2} s^{-1}$ measured at the bag surface by LiCor 850 quantum sensor (Licor, USA). The cultures were sparged with CO₂-air mixture (Table 1) at a rate of 5 L min^{-1} . After 8 days of P starvation, the culture was harvested and re-suspended in the same volume of complete Tamiya medium that contained a rich phosphate supplement during which the P-uptake and storage were followed.

The pre-cultures of *Desmodesmus* sp. and *A. obliquus* 46 were grown in flasks on BG-11 medium at 40 μ mol PAR photons $m^{-2} s^{-1}$ without bubbling. The pre-cultures were kept

at the exponential phase by daily dilution with the medium. The cultures of *Desmodesmus* sp. and *A. obliquus* 46 were initiated in complete BG-11 medium (+N) or nitrogen-lacking BG-11₀ medium (-N) (Rippka et al. 1979) in glass columns (6 cm internal diameter, 1.5 L volume). The cultures were grown under continuous illumination of 480 $\mu\text{mol PAR photons m}^{-2} \text{ s}^{-1}$ by a white light emitting diode source measured as described above in a temperature-controlled water bath at 27 °C and constant bubbling with air and/or CO₂ (see Table 1) at a rate of 0.3 L min⁻¹.

Electron microscopy

The microalgae samples for TEM were prepared with the standard protocol: fixed in 2 % *v/v* glutaraldehyde solution in 0.1 M sodium cacodylate buffer (pH 6.8–7.2, depending in the culture pH) at room temperature for 0.5 h and then post-fixed for 4 h in 1 % (*w/v*) OsO₄ in the same buffer. The samples, after dehydration through graded ethanol series including anhydrous ethanol saturated with or without uranyl acetate, were embedded in araldite. The samples for TEM in certain experiments were prepared according to protocols for high-pressure freezing and freeze-substitution with cryofixation without cryoprotectants or with 20 % BSA (bovine serum albumin). The cells were cryofixed in high-pressure freezing machine (Leica EM HPM100; Leica Microsystems, Austria). Frozen specimens were transferred to automatic freeze-substitution machine (Leica EM AFS2; Leica Microsystems, Austria) and placed in the substitution cocktail of 1 % OsO₄, 2 % glutaraldehyde, 1 % H₂O in acetone pre-cooled to -90 °C. The following protocol was used for freeze-substitution: -90 °C for 12 h; -90 °C to -60 °C within 8 h, -60 °C for 12 h, -60 °C to -30 °C within 8 h, -30 °C for 12 h, -30 °C to 0 °C within 8 h. At 0 °C, the specimens were rinsed thrice with precooled dry acetone then warmed up to room temperature over 2 h. Specimens were rinsed again at room temperature and embedded in EMbed 812 Resin (Electron Microscopy Sciences, USA). Ultrathin sections were made with an LKB-8800 (LKB, Sweden) ultratome, mounted to the formvar-coated TEM grids, and stained with lead citrate according to Reynolds (1963) and examined under JEM-1011 (JEOL, Tokyo, Japan) microscope.

The samples for nanoscale elemental analysis in analytical TEM using EDX and EELS were fixed, dehydrated, and embedded in araldite or EMbed 812 Resin (Electron Microscopy Sciences, USA) as described above usually excepting the staining with uranyl acetate and lead citrate. Semi-thin and ultrathin sections were made with a LKB-8800 (LKB, Sweden) ultratome and examined under JEM-2100 (JEOL, Japan) microscope equipped with a LaB₆ gun at the accelerating voltage 200 kV. Point EDX spectra were recorded using JEOL bright-field scanning TEM (STEM) module and X-Max X-ray detector system with ultrathin window capable of analysis of light element starting from boron (Oxford Instruments, UK). The

energy range of recorded spectra was 0–10 keV with a resolution of 10 eV per channel. This range includes the peaks of major biogenic elements (C, N, O, P, Ca, Mg, S, K, Na, Cl; see the table in Online Resource 1). At least 10 cells per specimen were analyzed. Spectra were recorded from different parts of electron-dense inclusions (at least 35 measurements for each point) and from other (sub)compartments of microalgae cell (thylakoid membranes, pyrenoid, plastoglobuli, starch grains in chloroplast, mitochondrion, cytoplasmic oil bodies, and nucleus). Spectra were processed with INKA software (Oxford instruments, UK) and presented in a range 0.1–4 keV.

EELS analysis was performed on ultrathin sections using Gatan GIF Quantum ER spectrometer (Gatan, USA). EELS point spectra from the vacuolar inclusions were recorded in high-angle annular dark-field scanning transmission electron microscopy (HAADF-STEM) mode using Gatan 806 HAADF-STEM detector. The energy-loss range was 100–600 eV, which includes C, N, P, S, Ca, Cl, and O edges (see the table in Online Resource 2). Digital Micrograph software (Gatan, USA) was used for spectra processing. The background was approximated by a power-law function. N and P elemental mapping was carried out using energy-filtered TEM (EFTEM) 3-window method with a 15 eV energy selecting slit. Two pre-edge images at 374 and at 392 eV and one post-edge image at 412 eV were recorded for N-mapping, and two pre-edge images at 101 and at 123 eV and post-edge image at 150 eV for P mapping. The energy windows were chosen basing on the spectra to avoid overlap with other element edges. The objective aperture was 40 μm . The elemental distributions were calculated automatically using Digital Micrograph software after alignment of the obtained images using a power law as the background model. Specimen thickness was controlled to ensure that it did not exceed the optimal value for EFTEM (below 0.5λ , where λ is inelastic mean free path length for the chosen experimental conditions).

Electron tomography

The tomographic tilt series was obtained from semi-thin sections in the tilt range from -55 to +55 degrees. The Tomography software package (CiFi, Japan) was used for image series acquisition, alignment, reconstruction, and tomogram visualization. Filtered back projection algorithm was used for volume reconstruction. The reconstruction had inverted contrast in relation to the TEM image.

NMR spectroscopy

Samples for nuclear magnetic resonance (NMR) measurements were prepared by gentle suspension of pellets, obtained by centrifugation of microalga cells, in 0.6 ml of the corresponding growth medium lacking phosphorus. Ten percent D₂O was added to final solution in order to stabilize resonance

conditions. The ^{31}P -NMR spectra were acquired on a Bruker Avance 600 spectrometer (Bruker, Germany), operating at 242.94 MHz ^{31}P frequency. Spectra were acquired at 298 K with 8500–9000 scans and a repetition rate of 2 s. Chemical shifts are referenced with respect to 85 % H_3PO_4 . Spectra were processed by TopSpin 2.0 and Mnova NMR (Mestrelab Research, Santiago de Compostela, Spain) software.

DAPI staining

One microliter of 300 μM solution of 4',6-diamidino-2-phenylindole (DAPI) in methanol prepared from a 5 mg/mL stock DAPI for nucleic acid (Sigma, USA) staining in methanol was added (300 nM final concentration) to cell suspension in corresponding media. After 5 min of incubation, aliquots of the cell suspension were transferred in a 96-well transparent plate. The plate was read on the plate reader Infinite 200 Pro (Tecan, Switzerland) in the bottom-read mode, and DAPI fluorescence was measured using UV excitation (360 nm). The fluorescence spectra were recorded in the 450–645 nm and processed by Magellan (Tecan, Switzerland) software. The emission in the range 450–480 nm was assigned to the nucleic acid-DAPI complex and that in the range 500–550 nm—to PolyP-DAPI complexes (Omelon and Grynopas 2008). The fluorescence spectra of the same media without cells were used to subtract the background signal. The spectra were measured every 10 min for 4 h after the DAPI addition.

Results

Whole cell survey microscopy

The bulk of the cells from the nutrient-replete cultures of all studied microalgae at early or middle stationary phase retained ultrastructural integrity of their cell compartments (Fig. 1). Moreover, the cells contained chloroplasts with well-developed thylakoid membranes, mitochondria, ample ribosomes, and dictyosomes of the Golgi apparatus. Furthermore, the cells did not possess a large amount of lipid and/or carbohydrate reserves. These observations suggested that a vigorous assimilation and formation of the cell structural components took place under our experimental conditions.

The cytoplasm of the studied cells frequently harbored vacuoles (Fig. 1). Interestingly, in most of the vacuoles, tonoplast formed tight contacts with the outer membrane of mitochondria and/or the outer membrane of chloroplast and/or epichloroplast membrane structures (EMS) (Figs. 1 and 2). The EMS are formed by the outer membrane of chloroplast. The peculiar membrane structures designated as twirls were involved in the formation of the contacts protruding to the vacuole lumen (Fig. 2e, g).

Stress-induced reorganization of assimilatory and reserve (sub)compartment of the microalgal cells exemplified by *Desmodesmus* sp. was detailed in our previous works (Solovchenko et al. 2014, 2015, 2016a; Gorelova et al. 2015b; Baulina et al. 2016). A specific effect of extremely high CO_2 levels on the vacuoles was the invagination of both chloroplast membranes and thylakoids, in addition to the membrane twirls, into the vacuole lumen (Fig. 2f).

In the nitrogen-starving cells, the vacuoles formed contacts with oil bodies, in addition to the contacts with chloroplasts and mitochondria, regardless of irradiance or CO_2 concentration. At the site of contact, the matrix of the oil bodies formed intrusion of different electron density (see the TEM image in Online Resource 3) in the vacuolar lumen; the intrusion retained fragments of 4.4 ± 1.8 -nm-thick boundary layer (the tonoplast in the same samples was 8.3 ± 0.9 nm thick). The boundary layer fragments facing the vacuolar lumen were decorated with grain-like depositions resembling those on the inner side of the tonoplast.

The vacuole number in the cell varied in the organism-specific manner, modulated by the growth phase and cultivation conditions. Thus, under the same cultivation conditions (e.g., during luxury P uptake after P-starvation), vacuoles were found in 25–50 % of the studied cell sections of *C. vulgaris* C-1 whereas in *C. vulgaris* 256 or *P. kessleri* 251, the organelles were present in 85–90 % sections.

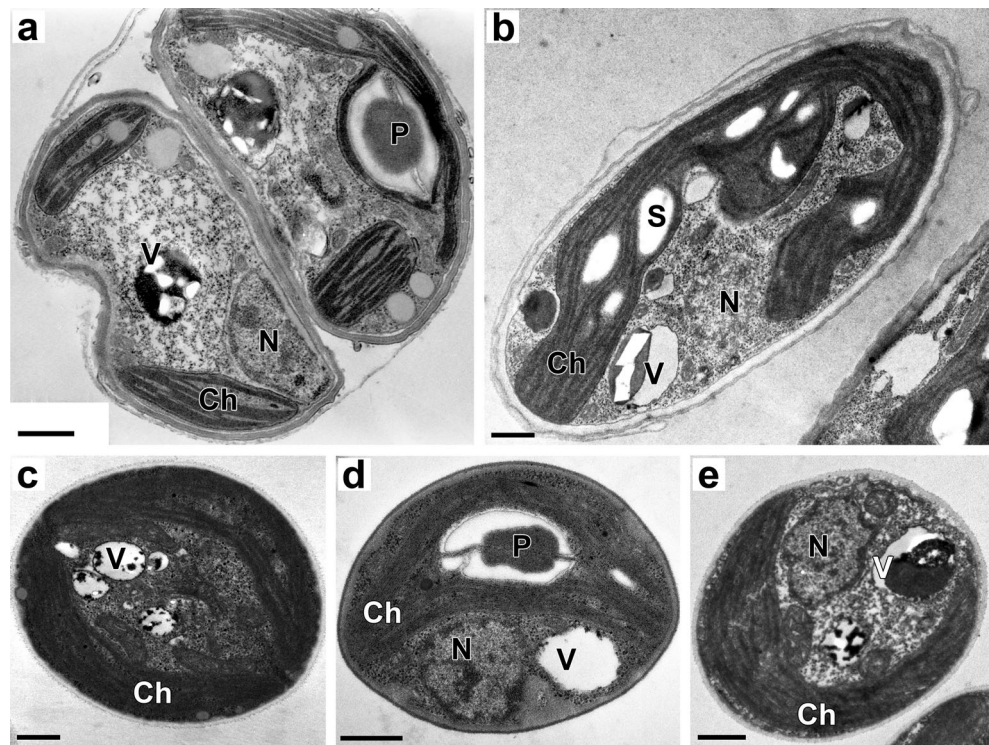
Almost all (90–100 %) sections of the *Desmodesmus* sp. cells contained vacuoles. In the course of cultivation at the atmospheric CO_2 level (sparging with air), the number of vacuoles per section declined upon reaching the stationary phase, approximately by 30 % regardless of nitrogen availability (Table 2). In the cultures of this microalga grown at 20 % CO_2 , the per section number of vacuoles did not depend on growth phase but increased twofold under N starvation (Table 2).

The vacuoles in the microalgal cells also differed in their size. The largest vacuoles were observed in the stationary-phase “100 % CO_2 , +N” cultures of *Desmodesmus* sp. (Table 2). The calculated vacuole area was in this case 2.5 or 4.4 times higher than in the cells grown at the atmospheric CO_2 or 20 % CO_2 , respectively. It is likely that the observed expansion of the vacuolar compartment was associated with the increase in the number of proton carriers sequestering H^+ from the cytoplasm into the vacuoles essential for maintenance of pH homeostasis during the acidification induced by excessive CO_2 inflow in the cell (Sasaki et al. 1999). In addition to the differences in size and number, the vacuoles differed considerably by their filling with inclusions and ultrastructural organization of the latter.

Morphology and ultrastructure of vacuolar inclusions

Assorted inclusions differing in their morphology and ultrastructure were distinctly observable against the featureless,

Fig. 1 The ultrastructure of the microalgae (TEM images, ultrathin cell sections stained with uranyl acetate and lead citrate). The cells from the nutrient-replete cultures at early or middle stationary phase retained the ultrastructural integrity of their compartments. The cytoplasm of the studied cells frequently harbored vacuoles. The vacuoles differed considerably by their filling with inclusions and ultrastructural organization of the latter. **a** *Desmodesmus* sp. IPPAS S-2014 from “Air, +N” culture. **b** *Acutodesmus obliquus* 46 from “20%CO₂, +N” culture. **c** *Chlorella vulgaris* CCALA 256 from “2.5%CO₂, +P” culture. **d** *Chlorella vulgaris* IPPAS C-1 from “2.5%CO₂, +P” culture. **e** *Parachlorella kessleri* CCALA 251 from “2.5%CO₂, +P” culture. *Ch* chloroplast, *N* nucleus, *P* pyrenoid, *S* starch grain, *V* vacuoles with different inclusions. Scale bars = 0.5 μm



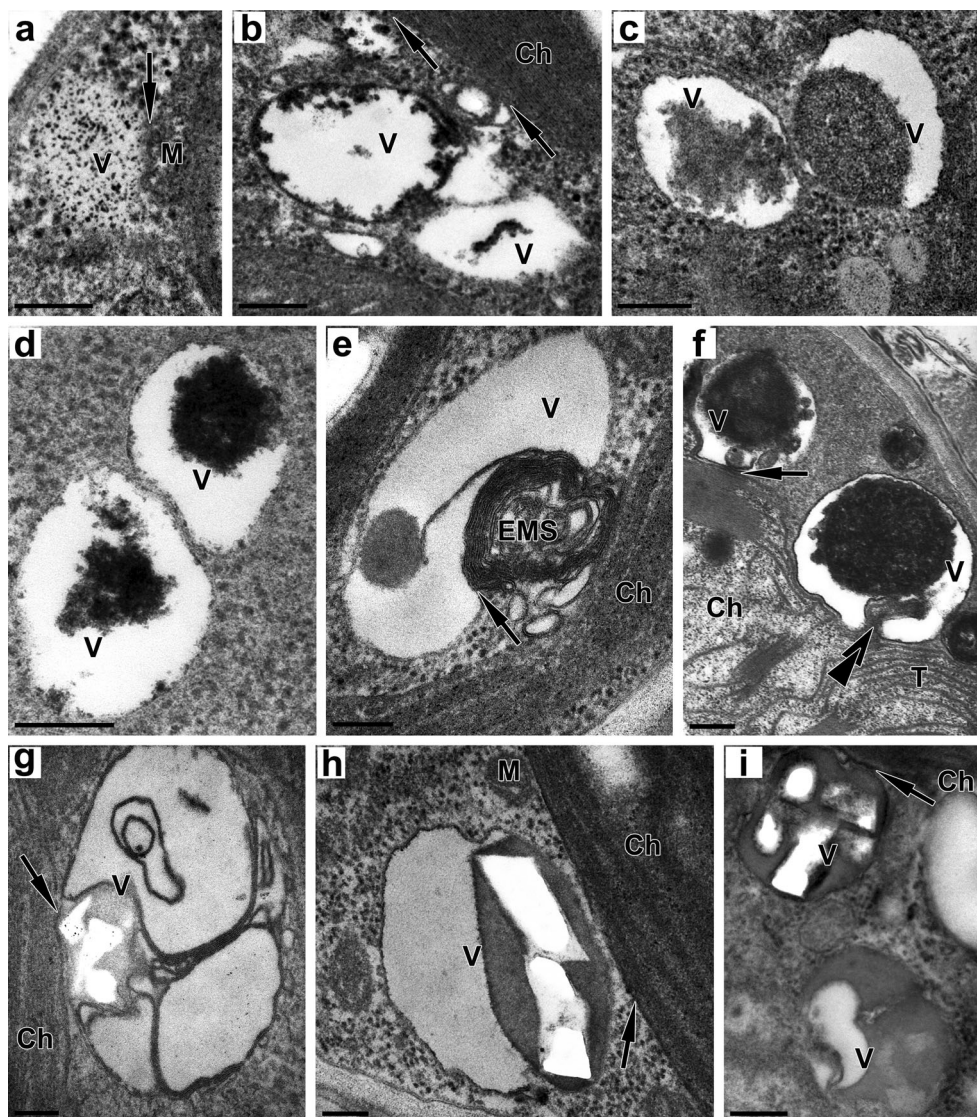
relatively electron-transparent background of the vacuolar matrix on the ultrathin cell sections stained with uranyl acetate (Figs. 2 and 3a, b). These inclusions could be divided into two categories: type I (granular) or type II (globular/crystalloid). The type I inclusions were represented by granules of high or moderate electron density. The small (4–22 nm) granules were scattered over the vacuole interior (Fig. 2a) or assembled on the inner side of the tonoplast (Fig. 2b–d, f–h). As a result, the latter assumed that the look of asymmetric membrane expanded to 10–13 nm. The granules often assembled in round-shaped porous clusters 200–1200 nm in diameter or clusters with uncertain shape (Fig. 2c–f). Noteworthy, the granular inclusions were normally in close contact with the internal surface of the tonoplast or the membrane structures intruding into the vacuole. Generally, the granular inclusions featured uneven electron density. The regions of the sample with extremely high electron density tended to crumble out and greatly complicated the analysis of fine structure of the inclusions; hence, it was revealed only in a limited number of regions. Nevertheless, we found that the granular inclusions featured an ordered structure comprised by peripheral spherules (Fig. 2b, d, f) and a core of rod- and/or round-shaped, linearly packed grains (Fig. 2c, d, f).

In certain experiments, the staining with uranyl acetate was omitted from the sample preparation of *C. vulgaris* 256, *C. vulgaris* C-1, or *P. kessleri* 251 cells; so, the overall electron density and contrast of the corresponding images were lower. Using this approach, we revealed that the inclusions incorporated large structurally ordered regions (Fig. 3c, d). In certain

parts, the section displayed interleaving (with a period of 4.90 ± 0.12 nm) mutually parallel patterns of low and high electron density of equal width arranged as individual wires in a multi-core cable. At a high magnification (Fig. 3d), the electron-dense regions composed of rows of electron-opaque granules arranged in a linear or zigzag fashion. These granules, arranged in series and interleaved by low-electron density matter, were connected by 1.64 ± 0.07 -nm-thick bridges, also of moderate electron density. The electron-dense rows occasionally extended to form local grain clusters, unordered or featuring a honeycomb-like pattern. Following the analogy of a multi-core cable, the latter pattern can be imagined as that formed by individual wires on the cross-section of the cable. In the latter case, the 5.07 ± 0.31 -nm grains were interconnected by several 1.31 ± 0.07 -nm-thick bridges of moderate electron density distinctly visible on the background of low electron density. It is conceivable that the images described above might reflect longitudinal, tangential, or transversal sections of parallel structures resembling beads (the electron-dense micelles) on a string embedded in an electron-transparent matter and twisted in the vacuolar interior.

The globular crystalloid (type II) inclusions were represented by globules of moderate electron density. The type II inclusions frequently contained mica-like crystalloid regions which often peeled off during the sample cutting resulting in the formation of electron-transparent regions with electron-dense borders (Figs. 2h, i and 3a, b). The type II inclusions were better preserved in semi-thin sections (Fig. 3e, f). The inclusions of both types (I and II) were often situated in the

Fig. 2 The ultrastructure of the microalgal vacuoles with inclusions (TEM images, ultrathin cell sections stained with uranyl acetate and lead citrate) of two types: granular type I (a–f) or globular/crystalloid type II (g–i). In most of the vacuoles, tonoplast formed close contacts with the outer membrane of mitochondria, chloroplast, and/or epichloroplast membrane structure intruding to the vacuole lumen. **a** *Chlorella vulgaris* IPPAS C-1 from “2.5 % CO₂, +P” culture. **b, d** *Chlorella vulgaris* CCALA 256 from “2.5 % CO₂, +P” culture. **c** *Parachlorella kessleri* CCALA 251 from “2.5 % CO₂, +P” culture. **e, g, h** *Acutodesmus obliquus* 46 from “20 % CO₂, +N” culture. **f, i** *Desmodesmus* sp. IPPAS S-2014 from “100 % CO₂, –N” culture and from “Air, +N” culture, respectively. *Ch* chloroplast, *EMS* epichloroplast membrane structure, *M* mitochondrion, *T* thylakoids, *V* vacuoles with different inclusions. *Arrows* point to the contacts of tonoplast with outer membrane of mitochondrial or chloroplast envelope and/or epichloroplast membrane structure. *Double arrowheads* point to the thylakoid and the chloroplast envelope intrusion to the vacuole lumen. *Scale bars* = 0.2 μm



same vacuole where they can be in close contact with or even penetrate to each other. The electron-opaque granules/spherules of the type I inclusions predominantly localized on the surface of type II globular inclusions and at the borders of the mica-like crystalloids (Figs. 2h and 3b, e, f).

Table 2 Vacuoles on the sections of the *Desmodesmus* sp. cell grown under different conditions

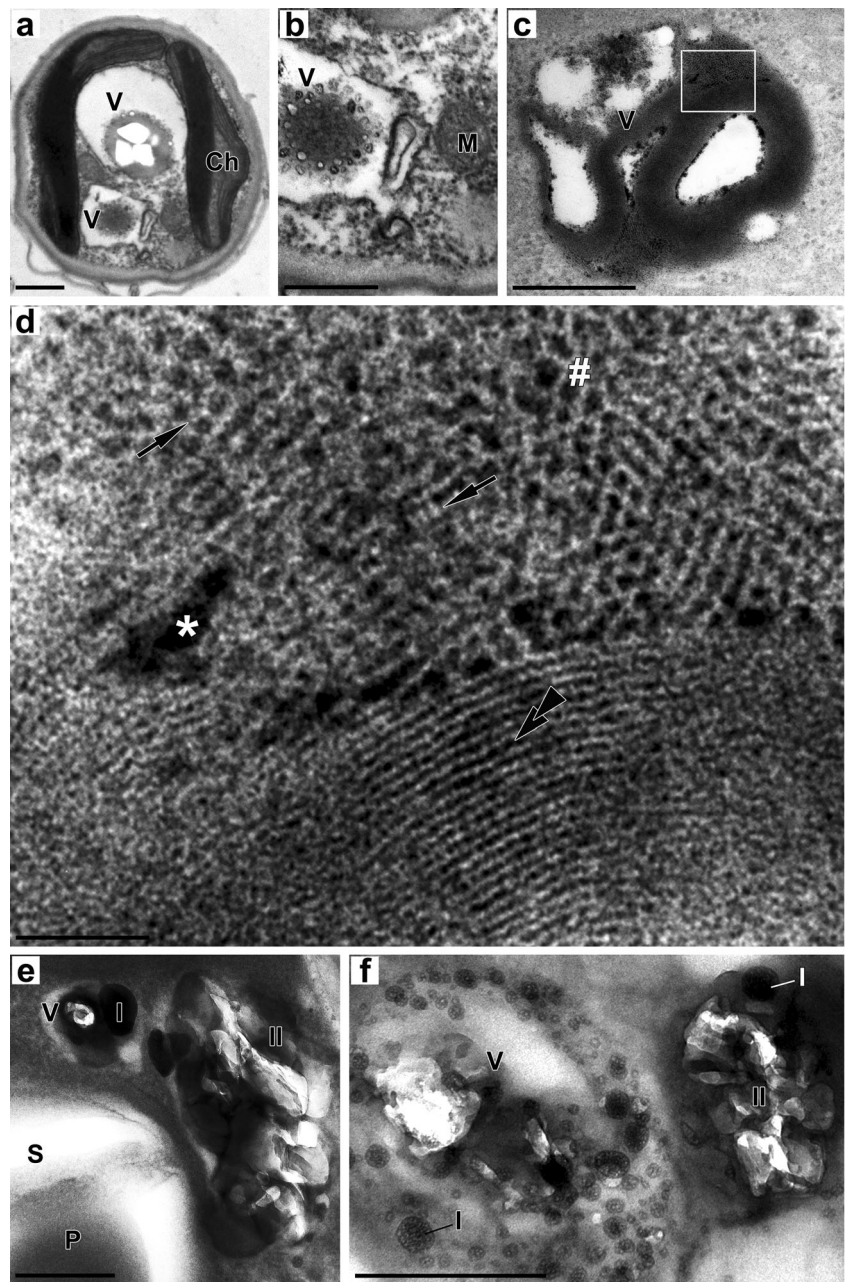
| Growth conditions | Vacuole number per section/total area, μm ² | |
|----------------------------|--|------------------------|
| | Early exponential phase | Early stationary phase |
| Air, +N | 6.0 ± 0.5/1.1 ± 0.1 | 3.6 ± 0.1/0.7 ± 0.1 |
| Air, –N | 5.3 ± 0.4/0.7 ± 0.1 | 3.0 ± 0.4/1.0 ± 0.2 |
| 20 % CO ₂ , +N | 3.7 ± 0.4/0.8 ± 0.1 | 3.8 ± 0.5/0.5 ± 0.1 |
| 20 % CO ₂ , –N | 8.6 ± 0.8/0.9 ± 0.4 | 7.5 ± 0.7/0.9 ± 0.2 |
| 100 % CO ₂ , +N | ND ^a | 3.9 ± 0.5/1.9 ± 0.4 |

^a Not determined

Apart from vacuoles, the small (20–90 nm) electron-dense spherules were revealed in the cytoplasm, e.g., of *C. vulgaris* C-1 cells; larger (40–230 nm) spherules of that type were found in the chloroplast stroma (see Online Resource 4). The spherules in the chloroplast stroma frequently formed close contacts with the stromal surface of the thylakoid. These structures resembled the type I vacuolar inclusions in their morphology and ultrastructure. The type I inclusions in the chloroplast stroma were revealed more clearly in the samples prepared according to the cryofixation-based protocol than in the samples made with the conventionally fixed samples (see Materials and methods and Online Resource 4). It is important that the electron tomography confirmed cytoplasmic localization of the electron-dense spherules making sure that they are not an artifact arising due to contamination of the sections by crumbled vacuolar content (Online Resources 5, 6).

However, the inclusions lacked a bilayer membrane separating them from the cytosol (or from the stroma) but

Fig. 3 The ultrastructure of the vacuolar inclusions of the studied microalgae (TEM images). *Desmodesmus* sp. IPPAS S-2014 cells from **a, b** the “100 % CO₂, +N” culture (ultrathin sections, uranyl acetate, and lead citrate staining) and **e, f** “+N” culture (semi-thin sections, no staining) are shown together with **c, d** *Chlorella vulgaris* CCALA 256 grown in “2.5%CO₂, +P” culture (ultrathin sections, stained with lead citrate, no uranyl acetate staining). **b, d** Enlarged fragments of **a** and **c**, respectively. *Ch* chloroplast, *I* type I inclusions, *II* type II inclusions, *M* mitochondrion, *P* pyrenoid, *S* starch grain, *V* vacuoles with different inclusions. *Double arrowheads* point to the region filled by the rows of electron-opaque granules forming a pattern designated as “multi-core cable” in the text. *Arrows* point to the bridges of moderate electron density connecting the rows of electron-opaque granules. *Asterisk* points to the local grain clusters. *Pound sign* (#) marks the site of electron-opaque granules arranged in the honeycomb-like pattern (designated in the text as “multi-core cable” cross-section pattern). *Scale bars* = 0.5 μm



possessed a boundary monolayer of intermediate electron density. The adjacent electron-dense granules often masked this boundary layer and complicated the measurement of its thickness (normally amounting to 1.8–5.9 nm). These structures harbored the electron-dense granules embedded into the substance of low electron density. The electron-dense granules within the sticks or spherules also featured 1.5-nm-thick boundary layer.

Elemental composition of the vacuolar inclusions

The EDX analysis of the vacuolar inclusions revealed their heterogeneity in terms of their elemental composition. Thus,

in all organisms studied, the type I inclusions contained regions enriched in P and O (Fig. 4a) whereas the type II inclusions possessed N-enriched regions (Fig. 4b). At the same time, the spectra of the surrounding vacuolar matrix lacked the characteristic X-ray peaks of P and N (Fig. 4c). Typical EDX spectra of semi-thin sections of the *Desmodesmus* sp. cells are shown in Fig. 4 (see also “Materials and methods”); similar spectra (not shown) were obtained for the other organisms studied under different cultivation conditions (Table 1). Hereinafter in EDX spectra, the peak of Cu is a peak from copper grid, the peaks of Si and Al—from components of equipment, the peaks of Os and U—from fixing and staining substances.

Generally, the maximal amplitude of the P peak was in the spectra taken from the type I vacuolar inclusions as well as from the electron-dense spherules localized in the cytoplasm or in the stroma of the chloroplasts (Online Resource 4e, f). Notably, P peaks of lower amplitude were discernible in the spectra from the nuclei (Fig. 4d). Since P peak normally overlapped with the peak of Os, the former peak was distinct only in the spectra from the cell regions highly enriched in P. The peaks of P in the EDX spectra of the type I inclusions were accompanied by a large peak of O and, as a rule, by the peaks of Ca and Mg. The peaks of P in the EDX spectra of the type I inclusions in the cells *Desmodesmus* sp., *A. obliquus* 46, *P. kessleri* 251 prepared by the conventional chemical fixation were seldom accompanied by a peak of S, whereas S was detected more frequently in the cryo-fixed cells of *C. vulgaris* C-1 (Online Resource 4f). In addition, the peaks of P in the EDX spectra of the type I inclusions in the *C. vulgaris* 256 and *P. kessleri* 251 cells were occasionally accompanied by an inconspicuous N peak (Online Resource 7).

The presence of inorganic P in the form of PolyP in the cell was independently confirmed using *in vivo* ^{31}P NMR spectroscopy (Fig. 5) or DAPI staining with subsequent recording of the fluorescence emission spectra (Fig. 6). Signals of inorganic PolyP have characteristic ^{31}P chemical shifts about -24 ppm, well distant from the signals of inorganic monophosphate (~ 1 ppm), sugar phosphate (~ 3 ppm), ATP, and NADP(H) (-6 to -14 ppm) (Sianoudis et al. 1986; Hebel et al. 1992).

The fluorescent dye DAPI is widely used to stain PolyP in cells *in situ* (Gomes et al. 2013). On the fluorescence emission spectra (Fig. 6), the amplitude of the band of PolyP-DAPI complex (530 nm) increased significantly after 15-min incubation with DAPI.

The characteristic peaks of N were presented in the spectra of the crystalloid matter as well as inhomogeneous matter of intermediate electron density (Fig. 3e, f and Fig. 4b). Notably, the peak of N from the type II vacuolar inclusions was much more pronounced than in the spectra from different cell structures expectedly rich in N such as nucleus, pyrenoid, or thylakoid membranes in the chloroplast (Fig. 4d–f). The point EDX spectra of starch grains, plastoglobuli, or cytoplasmic oil bodies did not present the peaks of P or N (Fig. 4g–j).

The peaks of C and O, the essential and ubiquitous elements of the cells, and the embedding medium were present in all EDX spectra regardless of cell structure, organism, or cultivation conditions, together with the peaks of the equipment components. The characteristic peaks of Na, Cl, or K were sporadically observed in the spectra of the vacuolar inclusions or from other cell compartments in *A. obliquus* 46. Although for *C. vulgaris* C-1 fixed with the cryofixation-based protocol, the peaks of Cl were constantly observed in the spectra from vacuolar inclusions, other cell compartments and the resin areas outside the cells. The signal of Cl most likely arises from a chlorine contaminant, which may be

contained in the EMbed 812 Resin used in our work for the embedding of cryo-fixed samples. It is known that contaminants in the medium may affect studies using the EDX: for example, Epon 812 contains a chlorine contaminant (Bagnell et al. 1995).

The EELS analysis carried out on the ultrathin sections confirmed the presence of P and O in the type I inclusions and N in the type II inclusions (see Online Resource 8). The EEL spectra did not reveal the signals only of P, N, C, and O probably due to low concentration of other elements and a high background signal.

Spatial distribution of P and N in the cell compartments

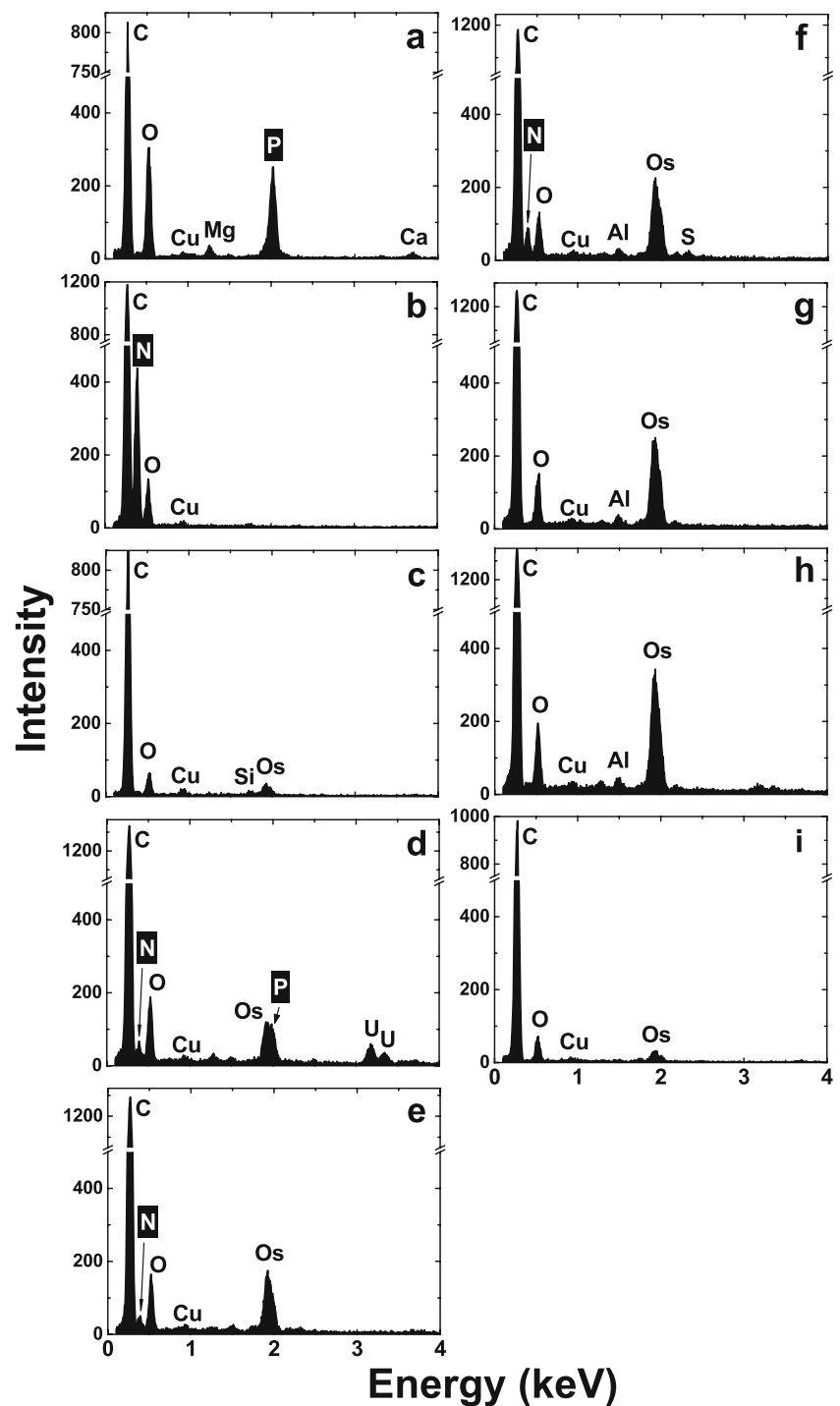
We compared the sections of the cells from the cultures at the same growth phase grown under different conditions (Table 1). The comparison revealed a striking difference both in the vacuolar content and predominant inclusion type. Thus, the exponential cultures of *Desmodesmus* sp. grown in the complete BG-11 medium sparged with air contained in the cell vacuoles clearly visible type I inclusions. These inclusions, vastly different in size (5–100 nm), were embedded in crystalloid or homogenous matter of intermediate electron density typical of the type II inclusions (Fig. 7a). The conspicuous peaks of P and O accompanied by Mg and Ca were present in the EDX spectra of the type I inclusions (Fig. 7b), while intensive peaks of N were revealed in the EDX spectra of the type II inclusions (Fig. 7c). In the cells from early stationary phase, the vacuoles were filled with the type II inclusions (Fig. 7d) featuring a pronounced peak of N in the EDX spectra (Fig. 7e). The type I inclusions enriched both in P and O were found only occasionally. A similar dynamics of the vacuolar inclusions was revealed in the cells of *A. obliquus* 46 (not shown).

On the EFTEM-based N maps obtained for the ultrathin sections of the cells from the exponential cultures grown in the complete medium (“Air, +N”) we observed nearly uniform distribution of the element over the cell section area (Fig. 8b, d). The bright objects on the P-maps corresponded to the type I inclusions (Fig. 8c, e) whereas no P signal from the other cell structures was detected.

On the N- and P-maps of the *Desmodesmus* sp. cells from the early stationary cultures grown in the N-replete medium, a pronounced signal of N was apparent in the regions of the thylakoids, pyrenoid, and type I inclusions despite poor preservation of the inclusions on the ultrathin slices (Fig. 8f–j). At the same time, there were only sporadic P-rich granules, and the P-signal was mainly emitted by other cell structures, e.g., chloroplast membranes and their twirls intruded into the vacuolar interior (Fig. 8h, j).

The cells from the exponential cultures of *Desmodesmus* sp. and *A. obliquus* 46 grown in the N-free medium (“Air, –N”) possessed vacuoles with the type I inclusions enriched in P and O, but only traces of N-rich type II inclusions. In the

Fig. 4 Typical point EDX spectra of vacuolar inclusions and various cell compartments *Desmodesmus* sp. IPPAS S-2014 grown in “+N” culture. Spectra were obtained in STEM-mode for semi-thin cell sections. **a** Vacuolar type I inclusion. **b** Vacuolar type II inclusion. **c** Vacuolar matrix surrounding inclusions. **d** Nucleus. **e** Thylakoids of chloroplast. **f** Pyrenoid. **g** Oil body. **h** Plastoglobule. **i** Starch grain. The main P reserve concentrates in the type I inclusion and the main N reserve—in the type II inclusion

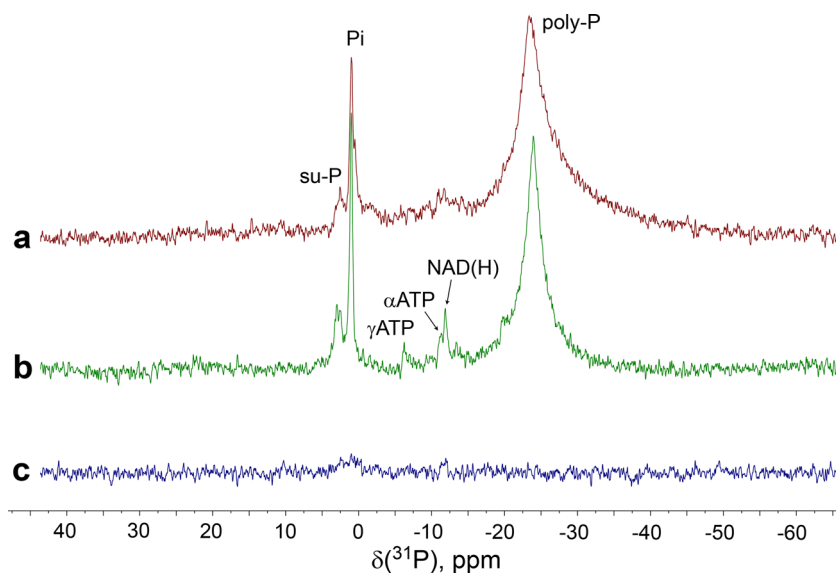


early stationary cells, a significant part of the vacuoles was occupied by P-rich type I inclusions, but no N-rich type II inclusion was found in the same cells. At the same time, multiple P-rich electron dense granules were revealed in cytoplasm (not shown).

A similar picture was observed in the cells grown in the presence of 100 % CO₂ (see Table 1). The cells of *Desmodesmus* sp. grown in the N-free medium sparged with elevated CO₂

possessed vacuoles with type I inclusion (Fig. 2f), at the same time in the complete medium possessed vacuoles with N-rich type II inclusions (Online Resource 9). On the EFTEM N-map obtained for the ultrathin section of the cell from culture grown in the complete medium, we observed that the N signal from the vacuolar type II inclusions was approximately 50 % higher than from other cell structures, e.g., thylakoids (Online Resource 9b, c). Summarizing the results of conventional and analytical

Fig. 5 ^{31}P -NMR spectra of *Desmodesmus* sp. IPPAS S-201 and *Chlorella vulgaris* IPPAS C-1 cell suspensions. **a** *Desmodesmus* sp. IPPAS S-201 with vacuoles, containing the type I inclusions (“20%CO₂, N +”). **b** *Chlorella vulgaris* IPPAS C-1 with vacuoles, containing the type I inclusions (“Air, P +”). **c** *Desmodesmus* sp. IPPAS S-201 cells lacking the type I inclusions (recorded after 8 days of P-starvation). *Pi* inorganic phosphate, *poly-P* polyphosphates, *su-P* sugar-phosphates



TEM, the PolyP type I inclusions can be described as structures resembling a multi-core cable formed by the strands of electron-opaque micelles (like individual “wires”) embedded in an electron-transparent matrix (resembling the cable “insulation”); these structures are obviously twisted and extruded to the vacuolar interior (Fig. 3c, d).

Discussion

Since the overwhelming majority of microalgae evolved in and hence adapted to oligotrophic environments, they are

naturally equipped to absorb and stockpile inside the cell as much nutrients (mostly P and N) as possible against future nutrient shortage. However, accumulation of the biogenic elements in the form directly bioavailable is not possible without a general disturbance of the cell metabolism. In particular, high levels of PolyP can be toxic in the cell (Gerasimaite et al. 2014) as well as N in the form of nitrate or ammonium when accumulated in the cytoplasm. Therefore, capacity of the cell for the nutrient reserves or cell nutrient quota is determined by the capacity of its storage compartments. The data accumulated in the literature, together with the findings of this work, indicate that vacuolar compartment accommodates a considerable part of N and P reserve of the cell. In particular, it plays a key role in accommodating reserves of P when this nutrient is ample in the surrounding of the microalgal cells.

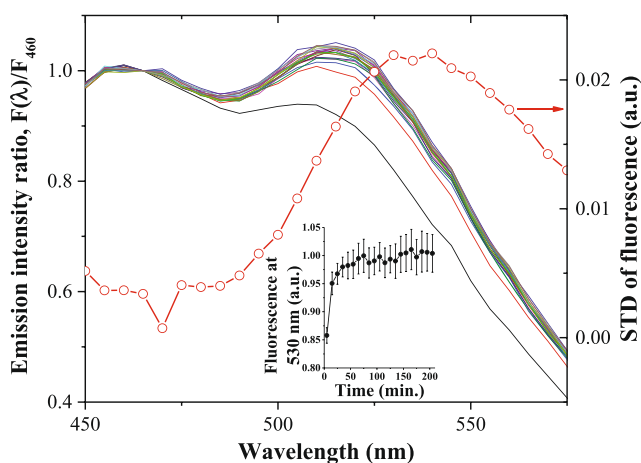


Fig. 6 The buildup of the UV-excited (360 nm) fluorescence emission of DAPI-stained cells of a P-sufficient culture “+N” of *Desmodesmus* sp. IPPAS S-2014. The fluorescence emission in the range 450–480 nm originates from nucleic acid-DAPI complex and that in the range 500–550 nm—from PolyP-DAPI complexes. The spectra normalized to 460 nm (the emission maximum of nucleic acid-DAPI complex) are shown. *Inset* the kinetics of fluorescence at 530 nm (the band of DAPI-stained polyphosphate emission). *STD* standard deviation (*red curve*, *right scale*)

Analytical TEM is a powerful method for studies of microalgae at the subcellular level

In the present work, we attempted to obtain a deeper insight into the role vacuolar compartment in the physiological plasticity of the microalgal cell. Toward this end, we employed several different free-living and symbiotic chlorophytes grown under very different cultivation conditions ranging from conducive for cell division to stressful. The diverse organisms and their growth conditions were complemented by an array of powerful analytical TEM techniques for the detection of biogenic elements. Below, we elaborate on the peculiarities of the analytical TEM application to research on microalgal cell compartment exemplified by vacuoles. After that, we outline how combination of these techniques with ultrastructural data elucidates the multi-faceted role of vacuoles in acclimation to stresses of different nature.

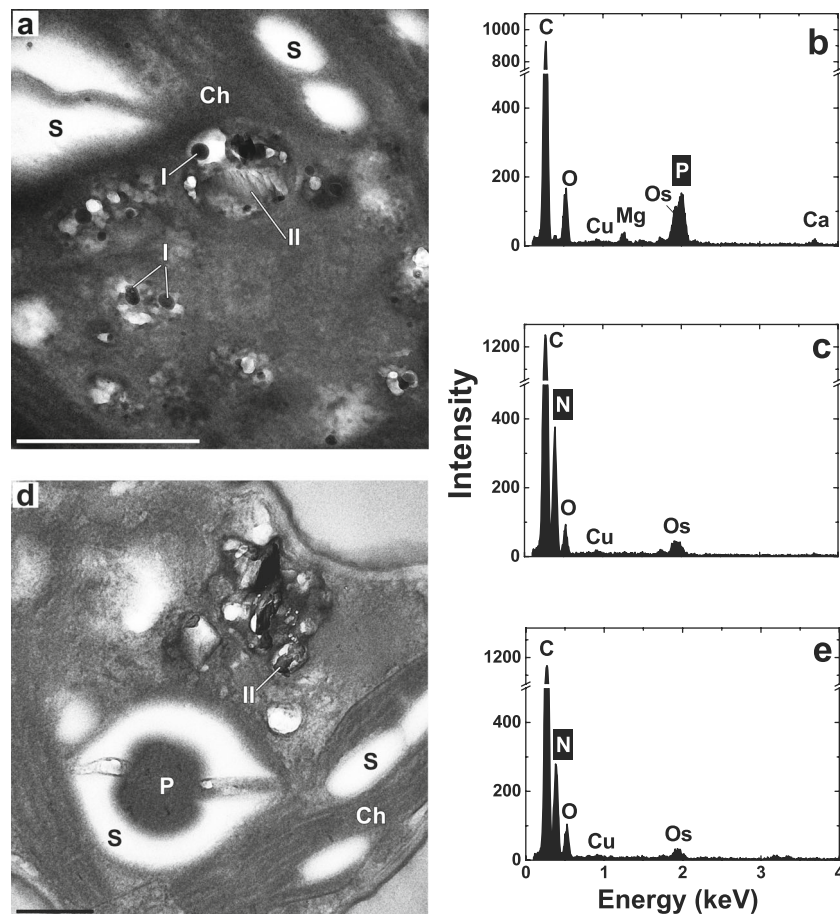


Fig. 7 Typical vacuolar inclusions in the cells of *Desmodesmus* sp. IPPAS S-2014 from **a–c** early exponential phase and **d, e** early stationary phase of the “Air, +N” cultures. **a, d** TEM images of semi-thin sections. **b, c, e** The point EDX spectra of the vacuolar inclusions. **a** On the early exponential phase, the vacuoles contained round-shaped porous clusters of type I inclusions embedded in crystalloid or homogenous matter of intermediate electron density of the type II inclusions. **b** Intensive peaks of phosphorus and oxygen in association with magnesium and calcium

are presented in EDX spectra from the type I inclusions. **c** Intensive nitrogen peak was revealed in the spectrum from the type II inclusion. **d** On early stationary phase, the cell vacuoles were filled with the type II inclusions. **e** The spectra from this inclusion type II displayed an intensive peak of N. Spectra were obtained for semi-thin sections from a point inside the compartment in STEM-mode. *Ch* chloroplast, *I* type I inclusions, *II* type II inclusions, *P* pyrenoid, *S* starch grain. Scale bars = 0.5 μm

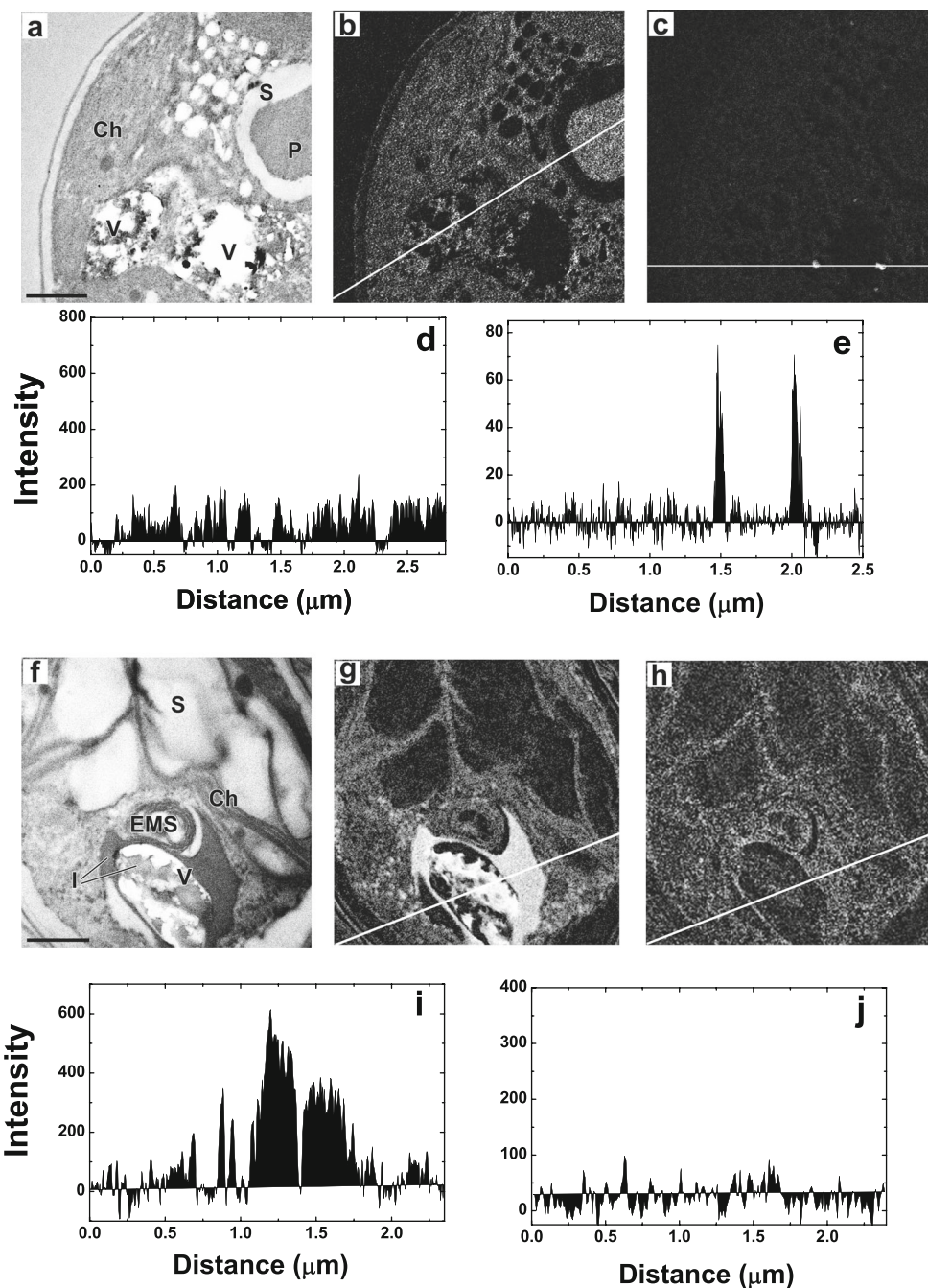
In the studies of microalgae, analytical TEM was, to the best of our knowledge, applied mainly to heavy metal quantification in the eco-toxicological context (Jensen et al. 1982; Nassiri et al. 1997; Nishikawa et al. 2003). In some works, EDX was used for confirmation of the presence of P in vacuolar compartment of microalgae such as *Scenedesmus obtusiusculus* (Tillberg et al. 1979, 1984), *Chlorella pyrenoidosa* (Adamec et al. 1979), *Chlamydomonas eugametos* (Siderius et al. 1996), and *Chlamydomonas reinhardtii* (Komine et al. 2000; Ruiz et al. 2001). Only recently, EDX spectroscopy was applied in an extensive research of PolyP accumulation in the cells *Parachlorella kessleri* NIES-2152 under S-depleted conditions (Ota et al. 2016).

A combination of analytical TEM and conventional ultrastructural techniques could be even more powerful in obtaining a deeper insight into microalgal physiology as exemplified by the vacuolar compartment in this work. Here, we

employed a stepwise approach starting from point EDX spectra revealing the elemental composition of the structure(s) of interest; then, we obtained EELS-based spatially resolved elemental maps showing distribution of the elements within the relevant compartments. Finally, we followed the changes in the subcellular distribution of the biogenic elements in response to different growth conditions. The results of analytical TEM methods provided quantitative information on the wide range of elements including light biogenic elements, spatially resolved at subcellular levels. It was consistent with and constituted a valuable complement to other methods of P detection used in this work such as ^{31}P NMR.

An important aspect of ultrastructural studies is prevention of artifacts readily arising at different stages, from cell fixation and section preparation and observation. We noticed that the vacuolar type I and type II inclusions frequently crumble during the ultrathin section preparation leading to poor

Fig. 8 EFTEM elemental mapping of *Desmodesmus* sp. IPPAS S-2014 cells from **a–e** early exponential and **f–j** early stationary phases of the “Air, +N” cultures. **a, f** TEM images of ultrathin sections of the cell area (no uranyl acetate and lead citrate staining). **b, g** EFTEM maps of N. **c, h** EFTEM maps of P. **d, i** profiles of the N maps. **e, j** profiles of the P maps. Bright inclusions (**c**) on the P maps correspond to the round granules. There was **g** a pronounced accumulation of N in the vacuoles but **h** no clear evidence of the presence of P-rich granules on early stationary culture cells. Profiles were recorded along the white lines (see the maps). *Ch* chloroplast, *EMS* epichloroplast membrane structure, *I* type II inclusions, *P* pyrenoid, *S* starch grain, *V* vacuole. Scale bars = 0.5 μm



preservation of vacuolar matter and contamination of the section surface resulting in false-positive detection of the inclusions. The electron tomography provided a necessary check for this showing that the P- and N-distributional data are essentially artifact-free and reflect the realistic picture of the nutrient localization in the microalgal cell compartments. This was crucial, e.g., for the reliable localization of the type I inclusions not only in the vacuoles and the cytoplasm, but also in the stroma of the chloroplasts. The PolyP granules in the chloroplasts of green microalgae

were observed earlier (Hase et al. 1963) including by ultra-cytochemical methods (Voříšek and Zachleder 1984).

Another important issue in TEM study of PolyP inclusions in the cell is the preservation of their native structure/composition, questionable in case of the conventional chemical fixation. This issue is even more important in spatially resolved studies pursuing to reveal the structure-function relations in a physiological context. Therefore, we paid close attention to comparative studies of chemical fixation and cryo-augmented fixation methods often praised for better preservation of the sample

nativity (Hurbain and Sachse 2011). Generally, we found no significant difference in the degree of preservation of the nutrient-rich inclusions in the cytoplasmic compartments (vacuoles). The only exception was comprised by the type I inclusions in the chloroplast stroma which were preserved better after the cryofixation-based protocols than after the standard chemical-fixation protocol.

Another helpful approach is the preparation of semi-thin sections which provides preservation of the vacuolar matter. An added benefit of this is increased sensitivity of the element analysis in bio-samples using EDX at high (100–400 kV) accelerating voltages in comparison with conventional thin sections (Nagata 2004). However, the semi-thin sections can hardly be used for resolving the structural information and should be combined for this purpose with the conventional thin section microscopy.

Vacuole is an important compartment for the nutrient logistics in the microalgal cell

Being better equipped with the analytical TEM methods, we revisited the structure and function of vacuolar compartment in the chlorophyte cells with a particular focus on P (PolyP) and N reserves. The cells of all studied microalgae displayed a vast diversity of vacuoles, which differed in size, morphology, fine structure, predominant element (P or N) content, and distribution depending on the strain, culture conditions, and growth phase. Still, the vacuoles containing reserves of P were present in all studied microalgae grown in P-replete media (Table 1).

The predominant form of vacuolar P reserve was PolyP apparent as type I vacuolar inclusions (Figs. 2, 3, 4, 7, Online Resource 7). However, the type I inclusions were also found in the chloroplast stroma and in the cytoplasm (Online Resource 4). Interestingly, strong buildup of the type I inclusions was observed under co-limitation conditions. In this work, it was recorded in N-starving cells (Figs. 2f, Online Resource 5); Ota et al. (2016) found a similar level of PolyP accumulation in sulfur-deprived cells of *Parachlorella kessleri* NIES-2152. It is conceivable that any limitation or stressor slowing down cell division will also slow down the consumption of P for synthesis of new cell building blocks such as phospholipids and nucleic acids. This can lead in re-partitioning of P taken up by the cell toward PolyP biosynthesis and hence to the enhanced accumulation of the type I inclusions.

An interesting finding of this work is a potential function of microalgal cell vacuoles as a depot of N reserves, e.g., in *Desmodesmus* sp. or *A. obliquus* 46 cells grown in N-replete media. Co-accumulation of N and P was documented in vacuoles of micorrhizal fungi cells (Bücking et al. 1998) where PolyP granules were suggested to have a high binding capacity for N. EELS and EFTEM were successfully applied to localize cyanophycin granules harbored by cyanobacterial cells as a N reserve (Koop et al. 2007). However, the literature

available at the time of this research lacked reports on large N reserves in microalgal cell vacuoles except a small amount of N associated with PolyP in *P. kessleri* NIES-2152 cells (Ota et al. 2016) and the amine accumulation in the acidic vacuoles of halotolerant alga *Dunaliella salina* in response to amine-induced alkaline stress (Pick et al. 1991).

The N reserves were associated mostly with the globular/crystalloid type II inclusions. The crystalloid inclusions in green microalgae can be of diverse nature. The crystalline cell inclusions identified as calcium oxalate, calcium carbonate, or protein-containing inclusions found in 45 species of Cladophorophyceae (Chlorophyta) (Leliaert and Coppejans 2004). However, in our work, the magnitude of the N signal from the crystalloid type II vacuolar inclusions in the EFTEM-map of N was at least three times higher than the signal from protein-rich compartments such as chloroplast thylakoids (Fig. 8f, g, i, Online Resource 9b, c) and pyrenoid (data not shown). These findings allow us to suggest that the bulk of the type II inclusions is more likely composed of polyamines than of proteins. Although we were unable to find reliable evidence of polyamine localization in the microalgal cell vacuoles in the literature available to us at the time of this writing, one may think that the vacuolar polyamines in microalgae are involved in the maintenance of the cell homeostasis as in many different organisms (Kusano et al. 2008).

Remarkably, the EDX spectra of the PolyP-enriched type I inclusions in *C. vulgaris* 256 and *P. kessleri* 251 featured a pronounced signal of N commensurate to that in the spectra from pyrenoids or thylakoids. It is likely that the presence of N in the type I inclusions suggests that these inclusions incorporate proteins. Nassiri et al. (1997) supposed that the presence of N and S in osmiophilic vesicles together with cadmium in *Tetraselmis suecia* grown in cadmium-contaminated medium indicated the presence of heavy metal-binding polypeptides. According to Nassiri et al. (1997), these polypeptides might trap pollutants, reducing the concentration of cytosolic free-metal ions. In our work, we propose that proteins in type I inclusions are likely the enzymes involved in synthesis, transport, and catabolism of PolyP.

Ultrastructural manifestations of the involvement of the vacuole in the synthesis and catabolism of PolyP in microalgae

Summarizing the data on the localization and ultrastructural organization of the type I inclusions, one can conclude that the synthesis and assembly of the electron-dense granules might be tightly associated with the tonoplast membrane. This suggestion is compatible with the observed pattern of the electron-dense grain deposition and aggregation on the inner surface of the tonoplast and the EMS membrane intrusion into the vacuole.

In view of these findings, it is possible to speculate that a coupled synthesis and translocation of PolyP take place in the microalgal cell vacuoles in a manner similar to that described in the yeast acidocalcisomes. The latter rely upon the vacuolar transporter chaperone (VTC) complex—endogenous vacuolar PolyP polymerase, Vtc4 (Gerasimaite et al. 2014; Hothorn et al. 2009; Müller et al. 2002, 2003). The suggested involvement of a VTC (affecting the vacuole fusion, see Müller et al. 2002) is indirectly supported by frequently observed fusions of the tonoplast with mitochondrial or plastidial envelope, EMS, or oil bodies' monolayer. Notably, VTC homologs were recently annotated by us in the *C. vulgaris* C1 and the *Desmodesmus* sp. transcriptomes (manuscript in preparation).

We hypothesize that activity of the putative VTC-like complex (the rate and continuity of the PolyP chain synthesis/translocation) determines the packing of the granules in the type I vacuolar inclusion complex. Thus, fast “pulsing” activity of the VTC-like complex might yield short-chained rods; a less frequent pulsation might give rise to the spherules described above (Figs. 2a, f and 3f). Continuous synthesis of the PolyP chains probably yields the characteristic “multi-core cable” pattern (see above) in the low electron-density sheath. When the synthesis of the PolyP chain is terminated, it is sealed at the ends with the low electron-density matter resulting in formation of the “bridges” shown in Fig. 3d. The complete and sealed PolyP chain is squeezed to the vacuolar lumen. Basing on the elemental composition data, we ruled out starch and sugars as the sealing matter (see also Ota et al. 2016), which is more likely represented by poly-(R)-3-hydroxybutyrate, PHB (Reusch 2000). Finally, the ordered pattern of the type I inclusion suggests the existence of multiple closely grouped VTC-like and PHB-synthesizing complexes.

Another important function of microalgal vacuoles is catabolism (Komine et al. 2000; Becker 2007; Yagisawa et al. 2009) of plastid proteins (Park et al. 1999) and PolyP as was shown for the halotolerant alga *Dunaliella salina* (Pick and Weiss 1991; Weiss et al. 1991). Under our experimental conditions, the type I inclusions in cells of vigorously dividing *Desmodesmus* sp. cultures were exhausted before the onset of the stationary phase suggesting that the PolyP-rich type I inclusions could be metabolized to cover the biosynthetic demand of P suggesting an important role of the lytic function of the vacuole in catabolism of PolyP.

Indeed, the PolyP-rich vacuoles of *Ch. reinhardtii* resemble lysosomes in their acidic pH (Komine et al. 2000) and presence of the enzymatic machinery for P_i transformation and exchange (H^+ -pumping PP_i -ase (Becker 2007), V-ATPase (Ruiz et al. 2001), and acid phosphatase (Matagne et al. 1976)). The vacuoles described in our work also had some traits in common with acidocalcisomes of *Ch. reinhardtii*, the electron-dense acidic organelles enriched with inorganic P and divalent cations (Docampo et al. 2005; Docampo and Huang 2016; Ruiz et al. 2001), namely the presence of the type I inclusions and their tentative lytic function. At the same time, the vacuoles of the

studied organisms differed from the acidocalcisomes by a peculiar pattern of P-rich type I inclusions resembling a multi-core cable (see Fig. 3c, d) and, in certain cases, by their presence of the N-rich type II inclusions.

The stressed microalgal cells often displayed a characteristic pattern of ultrastructural changes presumably related to the lytic function of their vacuolar compartment. In particular, their tonoplast often formed close contacts with the outer membrane of the chloroplast envelope and/or with the EMS (see Figs. 1 and 2). The close contacts are thought to facilitate the exit of vacuolar hydrolases (proteases) outside the vacuole to participate, e.g., in the decomposition of chloroplast (Wittenbach et al. 1982) or its components such as Rubisco (Minamikawa et al. 2001).

The characteristic intrusions of chloroplast into vacuolar lumen (designated as twirls) formed by the envelope (EMS) or, under more severe stresses (e.g., extremely high CO_2), by a larger part of the chloroplast containing thylakoids can also be a manifestation of the chloroplast decomposition. These changes in the topology of the vacuolar and chloroplast compartment rearrangements can result in the exposure of the chloroplast membrane lipids and proteins to the vacuolar hydrolases and hence in their accelerated turnover. Another characteristic change in the vacuolar membrane topology was constituted by formation of close contacts between tonoplast and mitochondria resulting presumably in acquisition of energy (via re-routing of ATP/ P_i fluxes) for hydrolysis, synthesis, and transport of the intra-vacuolar polymers. In the N-starving microalgal cells studied in this work, we also found close contacts or even blending of the vacuoles and cytoplasmic oil bodies. Most likely, these contacts are involved in catabolism and/or remobilization of the oil body lipids.

Conclusion

In conclusion, we demonstrated that the analytical TEM data in combination with ultrastructural study allow to investigate, on one hand, changes in cell morphology and structure in response to environmental stimuli and developmental stages and, on the other hand, functional differentiation of the vacuolar inclusions at subcellular level. The different inclusion types possess different functionalities: the type I inclusions are responsible mostly for storage of P in form of PolyP whereas the type II inclusions—for N storage in cell.

The microalgae cell vacuoles are multi-functional compartments serving as (1) a main depot of N and P in the cell including the synthesis and sequestration of PolyP; (2) site of the membrane lipid decomposition/turnover; (3) the energy and metabolite exchange between chloroplasts and mitochondria. These processes might play a significant role in acclimation in different stresses including N-starvation and extremely high level of CO_2 .

Acknowledgments The electron microscopy studies including analytical TEM were carried out at the User Facilities Center of M.V. Lomonosov Moscow State University and funded by Russian Foundation for Basic Research (grants 15-54-06004, 15-34-20096). High-pressure freezing and freeze-substitution of microalgal samples were performed in research resource center «Molecular and cell technologies» of St. Petersburg State University. Cultivation of the microalgae was supported by Russian Science Foundation (grant 14-50-00029). The dedicated assistance of Dr. Larisa Semenova, Dr. Irina Selyakh, and Mr. Pavel Scherbakov with cultivation of microalgae and Mr. Oleg Savelyev with measurements of NMR spectra is gratefully appreciated.

References

- Adamec J, Peeverly JH, Parthasarathy MV (1979) Potassium in polyphosphate bodies of *Chlorella pyrenoidosa* (chlorophyceae) as determined by x-ray microanalysis. *J Phycol* 15:466–468. doi:10.1111/j.1529-8817.1979.tb00721.x
- Aronova MA, Leapman RD (2012) Development of electron energy-loss spectroscopy in the biological sciences. *MRS Bull* 37:53–62. doi:10.1557/mrs.2011.329
- Bagnell R, Langaman C, Madden V, Suzuki K (1995) Ultrastructural methods for neurotoxicology and neuropathology. In: Neurotoxicology. Elsevier, pp 81–98.
- Baulina O, Gorelova O, Solovchenko A, Chivkunova O, Semenova L, Selyakh I, Scherbakov P, Burakova O, Lobakova E (2016) Diversity of the nitrogen starvation responses in subarctic *Desmodesmus* sp. (Chlorophyceae) strains isolated from symbioses with invertebrates. *FEMS Microbiol Ecol*. doi: 10.1093/femsec/fiw031
- Becker B (2007) Function and evolution of the vacuolar compartment in green algae and land plants (Viridiplantae). In: International Review of Cytology. Elsevier, pp 1–24.
- Bethmann B, Thaler M, Simonis W, Schonknecht G (1995) Electrochemical potential gradients of H^+ , K^+ , Ca^{2+} , and Cl^- across the tonoplast of the green alga *Eremosphaera viridis*. *Plant Physiol* 109:1317–1326
- Brydson R, Brown A, Benning LG, Livi K (2014) Analytical transmission electron microscopy. *Rev Mineral Geochem* 78:219–269. doi:10.2138/rmg.2014.78.6
- Bücking H, Beckmann S, Heyser W, Kottke I (1998) Elemental contents in vacuolar granules of ectomycorrhizal fungi measured by EELS and EDXS. A comparison of different methods and preparation techniques. *Micron* 29:53–61. doi:10.1016/S0968-4328(97)00059-0
- Burgos A, Maldonado J, De Los Rios A, Solé A, Esteve I (2013) Effect of copper and lead on two consortia of phototrophic microorganisms and their capacity to sequester metals. *Aquat Toxicol* 140–141:324–336. doi:10.1016/j.aquatox.2013.06.022
- Darehshouri A, Lütz-Meindl U (2010) H_2O_2 localization in the green alga *Micrasterias* after salt and osmotic stress by TEM-coupled electron energy loss spectroscopy. *Protoplasma* 239:49–56. doi:10.1007/s00709-009-0081-4
- Docampo R, Huang G (2016) Acidocalcisomes of eukaryotes. *Curr Opin Cell Biol* 41:66–72. doi:10.1016/j.ceb.2016.04.007
- Docampo R, de Souza W, Miranda K, Rohloff P, Moreno SN (2005) Acidocalcisomes conserved from bacteria to man. *Nat Rev Microbiol* 3:251–261. doi:10.1038/nrmicro1097
- Eder M, Lütz-Meindl U (2008) Pectin-like carbohydrates in the green alga *Micrasterias* characterized by cytochemical analysis and energy filtering TEM. *J Microsc* 231:201–214. doi:10.1111/j.1365-2818.2008.02036.x
- Eder M, Lütz-Meindl U (2010) Analyses and localization of pectin-like carbohydrates in cell wall and mucilage of the green alga *Netrium digitus*. *Protoplasma* 243:25–38. doi:10.1007/s00709-009-0040-0
- Egerton RF (2009) Electron energy-loss spectroscopy in the TEM. *Rep Prog Phys* 72:016502. doi:10.1088/0034-4885/72/1/016502
- Gerasimaite R, Sharma S, Desfougeres Y, Schmidt A, Mayer A (2014) Coupled synthesis and translocation restrains polyphosphate to acidocalcisome-like vacuoles and prevents its toxicity. *J Cell Sci* 127:5093–5104. doi:10.1242/jcs.159772
- Gomes FM, Ramos IB, Wendt C, Girard-Dias W, De Souza W, Machado EA, Miranda K (2013) New insights into the in situ microscopic visualization and quantification of inorganic polyphosphate stores by 4', 6-diamidino-2-phenylindole (DAPI)-staining. *Eur J Histochem* 57:227–235. doi:10.4081/ejh.2013.e34
- Gong Y, Hu H, Gao Y, Xu X, Gao H (2011) Microalgae as platforms for production of recombinant proteins and valuable compounds: progress and prospects. *J Ind Microbiol Biotechnol* 38:1879–1890. doi:10.1007/s10295-011-1032-6
- Gorelova O, Baulina O, Solovchenko A, Chekanov K, Chivkunova O, Fedorenko T, Lobakova E (2015a) Similarity and diversity of the *Desmodesmus* spp. microalgae isolated from associations with White Sea invertebrates. *Protoplasma* 252:489–503. doi:10.1007/s00709-014-0694-0
- Gorelova O, Baulina O, Solovchenko A, Selyakh I, Chivkunova O, Semenova L, Scherbakov P, Burakova O, Lobakova E (2015b) Coordinated rearrangements of assimilatory and storage cell compartments in a nitrogen-starving symbiotic chlorophyte cultivated under high light. *Arch Microbiol* 197:181–195. doi:10.1007/s00203-014-1036-5
- Hase S, Miyachi S, Mihara S (1963) A preliminary note on the phosphorus compounds in chloroplasts and volutin granules isolated from chlorella cells. In: Studies on microalgae and photosynthetic bacteria. University of Tokyo Press, Tokyo, p 619
- Hebeler M, Hentrich S, Grimme LH, Mayer A (1992) Phosphate regulation and compartmentation in *Chlamydomonas reinhardtii* studied by *in vivo* ^{31}P -NMR. In: Murata N (ed) Research in photosynthesis. Springer Netherlands, Dordrecht, pp 717–720
- Hedrich R, Kurkdjian A, Guern J, Flüggé UI (1989) Comparative studies on the electrical properties of the H^+ translocating ATPase and pyrophosphatase of the vacuolar-lysosomal compartment. *EMBO J* 8:2835–2841
- Hothorn M, Neumann H, Lenherr ED, Wehner M, Rybin V, Hassa PO, Uttenweiler A, Reinhardt M, Schmidt A, Seiler J, Ladurner AG, Herrmann C, Scheffzek K, Mayer A (2009) Catalytic core of a membrane-associated eukaryotic polyphosphate polymerase. *Science* 324:513–516. doi:10.1126/science.1168120
- Hurbain I, Sachse M (2011) The future is cold: cryo-preparation methods for transmission electron microscopy of cells. *Biol Cell* 103:405–420. doi:10.1042/BC20110015
- Jensen TE, Rachlin JW, Jani V, Warkentine B (1982) An x-ray energy dispersive study of cellular compartmentalization of lead and zinc in *Chlorella saccharophila* (Chlorophyta), *Navicula incerta* and *Nitzschia closterium* (Bacillariophyta). *Environ Exp Bot* 22:319–328. doi:10.1016/0098-8472(82)90024-7
- Komine Y, Eggink LL, Park H, Hooper JK (2000) Vacuolar granules in *Chlamydomonas reinhardtii*: polyphosphate and a 70-kDa polypeptide as major components. *Planta* 210:897–905. doi:10.1007/s004250050695
- Koop A, Voss I, Thesing A, Kohl H, Reichelt R, Steinbüchel A (2007) Identification and localization of cyanophycin in bacteria cells via imaging of the nitrogen distribution using energy-filtering transmission electron microscopy. *Biomacromolecules* 8:2675–2683. doi:10.1021/bm0611230
- Kusano T, Berberich T, Tateda C, Takahashi Y (2008) Polyamines: essential factors for growth and survival. *Planta* 228:367–381. doi:10.1007/s00425-008-0772-7
- Lam MK, Lee KT (2012) Microalgae biofuels: a critical review of issues, problems and the way forward. *Biotechnol Adv* 30:673–690. doi:10.1016/j.biotechadv.2011.11.008

- Leliaert F, Coppejans E (2004) Crystalline cell inclusions: a new diagnostic character in the Cladophorophyceae (Chlorophyta). *Phycologia* 43:189–203. doi:10.2216/i0031-8884-43-2-189.1
- Lourenço SO, Barbarino E, Marquez UML, Aidar E (1998) Distribution of intracellular nitrogen in marine microalgae: basis for the calculation of specific nitrogen-to-protein conversion factors. *J Phycol* 34:798–811. doi:10.1046/j.1529-8817.1998.340798.x
- Lütz-Meindl U, Lütz C (2006) Analysis of element accumulation in cell wall attached and intracellular particles of snow algae by EELS and ESI. *Micron* 37:452–458. doi:10.1016/j.micron.2005.11.004
- Maeshima M (2000) Vacuolar H⁺-pyrophosphatase. *Biochim Biophys Acta BBA - Biomembr* 1465:37–51. doi:10.1016/S0005-2736(00)00130-9
- Marty F (1999) Plant vacuoles. *Plant Cell* 11:587–600
- Matagne RF, Loppes R, Deltour R (1976) Phosphatase of *Chlamydomonas reinhardtii*: biochemical and cytochemical approach with specific mutants. *J Bacteriol* 126:937–950
- Millach L, Solé A, Esteve I (2015) Role of *Geitlerinema* sp. DE2011 and *Scenedesmus* sp. DE2009 as bioindicators and immobilizers of chromium in a contaminated natural environment. *BioMed Res Int* 2015: 1–11. doi:10.1155/2015/519769
- Minamikawa T, Toyooka K, Okamoto T, Hara-Nishimura I, Nishimura M (2001) Degradation of ribulose-bisphosphate carboxylase by vacuolar enzymes of senescing French bean leaves: immunocytochemical and ultrastructural observations. *Protoplasma* 218:144–153
- Müller O, Bayer MJ, Peters C, Andersen JS, Mann M, Mayer A (2002) The Vtc proteins in vacuole fusion: coupling NSF activity to V₀ trans-complex formation. *EMBO J* 21:259–269. doi:10.1093/emboj/21.3.259
- Müller O, Neumann H, Bayer MJ, Mayer A (2003) Role of the Vtc proteins in V-ATPase stability and membrane trafficking. *J Cell Sci* 116:1107–1115
- Nagata T (2004) X-ray microanalysis of biological specimens by high voltage electron microscopy. *Prog Histochem Cytochem* 39:185–319
- Nassiri Y, Wéry J, Mansot JL, Ginsburger-Vogel T (1997) Cadmium bioaccumulation in *Tetraselmis suecica*: an electron energy loss spectroscopy (EELS) study. *Arch Environ Contam Toxicol* 33: 156–161
- Nishikawa K, Yamakoshi Y, Uemura I, Tominaga N (2003) Ultrastructural changes in *Chlamydomonas acidophila* (Chlorophyta) induced by heavy metals and polyphosphate metabolism. *FEMS Microbiol Ecol* 44:253–259. doi:10.1016/S0168-6496(03)00049-7
- Omelon S, Grynopas M (2008) Relationships between polyphosphate chemistry, biochemistry and apatite biomineralization. *Chem Rev* 108:4694–4715. doi:10.1021/cr0782527
- Ota S, Yoshihara M, Yamazaki T, Takeshita T, Hirata A, Konomi M, Oshima K, Hattori M, Bišová K, Zachleder V, Kawano S (2016) Deciphering the relationship among phosphate dynamics, electron-dense body and lipid accumulation in the green alga *Parachlorella kessleri*. *Sci Rep* 6:25731. doi:10.1038/srep25731
- Park H, Eggink LL, Roberson RW, Hooper JK (1999) Transfer of proteins from the chloroplast to vacuoles in *Chlamydomonas reinhardtii* (Chlorophyta): a pathway for degradation. *J Phycol* 35:528–538. doi:10.1046/j.1529-8817.1999.3530528.x
- Pick U, Weiss M (1991) Polyphosphate hydrolysis within acidic vacuoles in response to amine-induced alkaline stress in the halotolerant alga *Dunaliella salina*. *Plant Physiol* 97:1234–1240
- Pick U, Zeelon O, Weiss M (1991) Amine accumulation in acidic vacuoles protects the halotolerant alga *Dunaliella salina* against alkaline stress. *Plant Physiol* 97:1226–1233
- Pittman JK, Dean AP, Osundeko O (2011) The potential of sustainable algal biofuel production using wastewater resources. *Bioresour Technol* 102:17–25. doi:10.1016/j.biortech.2010.06.035
- Powell N, Shilton A, Chisti Y, Pratt S (2009) Towards a luxury uptake process via microalgae – defining the polyphosphate dynamics. *Water Res* 43:4207–4213. doi:10.1016/j.watres.2009.06.011
- Ray K, Mukherjee C, Ghosh AN (2013) A way to curb phosphorus toxicity in the environment: use of polyphosphate reservoir of Cyanobacteria and microalga as a safe alternative phosphorus biofertilizer for Indian agriculture. *Environ Sci Technol* 47:11378–11379. doi:10.1021/es403057c
- Reusch RN (2000) Transmembrane ion transport by polyphosphate/poly-(R)-3-hydroxybutyrate complexes. *Biochem Mosc* 65:280–295
- Reynolds ES (1963) The use of lead citrate at high pH as an electron-opaque stain in electron microscopy. *J Cell Biol* 17:208–212
- Rippka R, Deruelles J, Waterbury JB, Herdman M, Stanier RY (1979) Generic assignments, strain histories and properties of pure cultures of Cyanobacteria. *J Gen Microbiol* 111:1–61. doi:10.1099/00221287-111-1-1
- Robinson DG, Hoppenrath M, Oberbeck K, Luykx P, Ratajczak R (1998) Localization of pyrophosphatase and V-ATPase in *Chlamydomonas reinhardtii*. *Bot Acta* 111:108–122. doi:10.1111/j.1438-8677.1998.tb00685.x
- Ruiz FA, Marchesini N, Seufferheld M, Govindjee DR (2001) The polyphosphate bodies of *Chlamydomonas reinhardtii* possess a proton-pumping pyrophosphatase and are similar to acidocalcisomes. *J Biol Chem* 276:46196–46203. doi:10.1074/jbc.M105268200
- Sasaki T, Pronina NA, Maeshima M, Iwasaki I, Kurano N, Miyachi S (1999) Development of vacuoles and vacuolar H⁺-ATPase activity under extremely high CO₂ conditions in *Chlorococcum littorale* cells. *Plant Biol* 1:68–75. doi:10.1111/j.1438-8677.1999.tb00710.x
- Sianoudis J, Küsel AC, Mayer A, Grimme LH, Leibfritz D (1986) Distribution of polyphosphates in cell-compartments of *Chlorella fusca* as measured by ³¹P-NMR-spectroscopy. *Arch Microbiol* 144:48–54. doi:10.1007/BF00454955
- Siderius M, Musgrave A, Ende H, Koerten H, Cambier P, Meer PVD (1996) *Chlamydomonas eugametos* (Chlorophyta) stores phosphate in polyphosphate bodies together with calcium. *J Phycol* 32:402–409. doi:10.1111/j.0022-3646.1996.00402.x
- Solovchenko A, Gorelova O, Selyakh I, Semenova L, Chivkunova O, Baulina O, Lobakova E (2014) *Desmodesmus* sp. 3Dp86E-1—a novel symbiotic chlorophyte capable of growth on pure CO₂. *Mar Biotechnol* 16:495–501. doi:10.1007/s10126-014-9572-1
- Solovchenko A, Gorelova O, Selyakh I, Pogosyan S, Baulina O, Semenova L, Chivkunova O, Voronova E, Konyukhov I, Scherbakov P, Lobakova E (2015) A novel CO₂-tolerant symbiotic *Desmodesmus* (chlorophyceae, desmodesmaceae): acclimation to and performance at a high carbon dioxide level. *Algal Res* 11: 399–410. doi:10.1016/j.algal.2015.04.011
- Solovchenko A, Gorelova O, Selyakh I, Baulina O, Semenova L, Logacheva M, Chivkunova O, Scherbakov P, Lobakova E (2016a) Nitrogen availability modulates CO₂ tolerance in a symbiotic chlorophyte. *Algal Res* 16:177–188. doi:10.1016/j.algal.2016.03.002
- Solovchenko A, Verschoor AM, Jablonowski ND, Nedbal L (2016b) Phosphorus from wastewater to crops: an alternative path involving microalgae. *Biotechnol Adv*. doi:10.1016/j.biotechadv.2016.01.002
- Sviben S, Gal A, Hood MA, Bertinetti L, Politi Y, Bennet M, Krishnamoorthy P, Schertel A, Wirth R, Sorrentino A, Pereira E, Faivre D, Scheffel A (2016) A vacuole-like compartment concentrates a disordered calcium phase in a key cocolithophorid alga. *Nat Commun* 7:11228. doi:10.1038/ncomms11228
- Tamiya H (1957) Mass culture of algae. *Annu Rev Plant Physiol* 8:309–334. doi:10.1146/annurev.pp.08.060157.001521
- Tillberg JE, Barnard T, Rowley J (1979) X-ray microanalysis of phosphorus in *Scenedesmus obtusiusculus*. *Physiol Plant* 47:34–38. doi:10.1111/j.1399-3054.1979.tb06508.x
- Tillberg J-E, Barnard T, Rowley JR (1984) Phosphorus status and cytoplasmic structures in *Scenedesmus* (Chlorophyceae) under different metabolic regimes. *J Phycol* 20:124–136. doi:10.1111/j.0022-3646.1984.00124.x
- Voříšek J, Zachleder V (1984) Redistribution of phosphate deposits in the alga *Scenedesmus quadricauda* deprived of exogenous phosphate—

- an ultra-cytochemical study. *Protoplasma* 119:168–177. doi:[10.1007/BF01288871](https://doi.org/10.1007/BF01288871)
- Warley A (2016) Development and comparison of the methods for quantitative electron probe X-ray microanalysis analysis of thin specimens and their application to biological material. *J Microsc* 261:177–184. doi:[10.1111/jmi.12306](https://doi.org/10.1111/jmi.12306)
- Weiss M, Bental M, Pick U (1991) Hydrolysis of polyphosphates and permeability changes in response to osmotic shocks in cells of the halotolerant alga *Dunaliella*. *Plant Physiol* 97:1241–1248
- Wittenbach VA, Lin W, Hebert RR (1982) Vacuolar localization of proteases and degradation of chloroplasts in mesophyll protoplasts from senescing primary wheat leaves. *Plant Physiol* 69:98–102
- Yagisawa F, Nishida K, Yoshida M, Ohnuma M, Shimada T, Fujiwara T, Yoshida Y, Misumi O, Kuroiwa H, Kuroiwa T (2009) Identification of novel proteins in isolated polyphosphate vacuoles in the primitive red alga *Cyanidioschyzon merolae*: novel proteins comprising polyphosphate vacuoles. *Plant J* 60:882–893. doi:[10.1111/j.1365-313X.2009.04008.x](https://doi.org/10.1111/j.1365-313X.2009.04008.x)